Environmental Science: Atmospheres

ROYAL SOCIETY OF CHEMISTRY

PAPER

View Article Online
View Journal | View Issue

Cite this: *Environ. Sci.: Atmos.*, 2025, **5**, 703

Seasonal analysis of organic aerosol composition resolves anthropogenic and biogenic sources at a rural background station in central Europe†

Markus Thoma, Franziska Bachmeier,‡ Karina Knauf, Julia David, Mario Simon and Alexander L. Vogel *

Received 17th December 2024
Accepted 5th May 2025

DOI: 10.1039/d4ea00163j

rsc.li/esatmospheres

Organic aerosol (OA) has a significant impact on Earth's climate and human health, while its chemical composition remains largely unknown. A detailed analysis of the chemical composition of particulate matter (PM) can identify origins, sources and transformation pathways and reveal mitigation potential for the anthropogenic organic fraction. Here, we follow a top-down molecular resolution approach of source attribution of organic compounds in $PM_{2.5}$ at a rural background station in central Europe. One year of PM filters were measured using ultra-high-performance liquid chromatography coupled to electrospray ionisation high-resolution Orbitrap mass spectrometry. Non-target analysis detected over 6000 compounds, which hierarchical cluster analysis separated into a biogenic and an anthropogenic compound cluster. Compounds of the biogenic cluster make up a large part of SOA during summer, indicating strong local influence by the vegetation. Anthropogenic compounds are relatively enriched during colder conditions, with temporarily strong transport of air pollution. Concentration-weighted trajectories show the air mass origins of these pollution events and allow for an interpretation of potential sources.

Environmental significance

Organic aerosol (OA) is a major constituent of fine particulate matter, highly complex in its chemical composition due to variable anthropogenic and biogenic emissions, their oxidative transformation, long-range transport of pollution, and multiphase chemistry. Meteorological processes and seasonal cycles influence the transport and concentration of aerosol particles at background stations. Detailed chemical characterisation of year-long organic aerosol composition at background sites allows for deciphering the anthropogenic and biogenic contribution to the total aerosol burden, and thus improve the understanding of the impact of organic aerosols of climate and human health.

1 Introduction

Outdoor air pollution, such as fine particulate matter ($PM_{2.5}$), has a major impact on the climate.[1] However, short-lived climate forcers are difficult to model due to their high spatial and temporal variability, resulting in large uncertainties in the effective radiative forcing of aerosols.[2] Furthermore, PM affects human health,[3] causing millions of premature deaths[4,5] and more than US$5 trillion in welfare losses every year.[6] Though the major fraction of submicron PM is from organic compounds,[7] their sources or organic precursor vapours, their atmospheric oxidation mechanisms and cross-reactions with inorganic trace gases remain unknown and are the focus of ongoing research. Volatile organic compounds (VOCs) of biogenic (BVOC) and anthropogenic (AVOC) origin can be oxidised by hydroxyl radicals (OH), ozone (O_3) and nitrate radicals (NO_3).[8] The oxidation leads to a higher functionality, which in turn reduces the volatility of the products, hence gas-to-particle conversion contributes to the formation of secondary organic aerosol (SOA) particles.[3] Chen *et al.*[9] estimate that in Europe 71% of organic aerosol is secondary in origin, while primary organic aerosol accounts for 16% and up to 21% in winter. Furthermore, Zhang *et al.*[10] estimate that 25% of the organic carbon in aerosols in the northern hemisphere is of fossil origin. In contrast to natural sources, this proportion can be reduced with suitable measures and thus mitigate the impacts on climate and health. The diverse physico-chemical properties of the generated SOA make universal measurement challenging,[11] and a comprehensive characterisation is not yet possible because each detection method and instrumentation has its limits. Therefore only a combination of measurement techniques can characterise the complex SOA composition.[12]

Institute for Atmospheric and Environmental Sciences, Goethe University Frankfurt, Altenhöferallee 1, 60438 Frankfurt, Germany. E-mail: vogel@iau.uni-frankfurt.de

† Electronic supplementary information (ESI) available. See DOI: https://doi.org/10.1039/d4ea00163j

‡ Present address: German Environmental Agency (Umweltbundesamt), Paul-Ehrlich-Straße 29, 63225 Langen, Germany.

Aerosol collection on filters using high-volume samplers (HVS) is a robust and straightforward approach for sampling and enrichment, even at remote stations and over long periods of time. Maximising the flowrate of HVS enables the extensive offline chemical analysis on a diurnal resolution or can even provide high-concentration extracts for toxicological studies.[13] Analysis by ultra-high-performance liquid chromatography (UHPLC) coupled to high-resolution mass spectrometry (HRMS) is a common method of measuring organic compounds in atmospheric filter samples. High-resolution and accurate-mass measurements allow the detection of unknown compounds in highly complex samples by non-targeted analysis (NTA).[14] Comparison of tandem mass spectrometry (MS^2) fragmentation spectra with databases such as mzCloud[15] for anthropogenic chemicals or the aerosolomics database for atmospheric oxidation products[16] provides a higher level of confidence in compound identification in atmospheric environmental samples.[17–20]

Another but much more complex method, mainly in terms of sample preparation, for distinguishing between anthropogenic-fossil and biogenic organic aerosol (OA) is the analysis of the ^{14}C to ^{12}C ratio in an accelerator mass spectrometer, such as the Mini Radiocarbon Dating System[21] (MICADAS), as fossil OA is depleted in ^{14}C.[22,23]

The use of a statistical approach such as hierarchical cluster analysis (HCA) is well suited to reducing the complexity of ambient aerosol fingerprints while also identifying compounds that follow similar trends.[16] In contrast to positive matrix factorisation (PMF), HCA cannot split individual signals into different factors. However, Ma *et al.*[24] have demonstrated that HCA can effectively resolve the seasonality of different organic aerosol composition classes in Beijing.

In this study we follow a top-down approach to identify sources and transformation pathways of SOA, based on the chemical characterisation of ambient filter samples. Therefore, we analysed 352 samples and 49 field blanks collected over one year at the Taunus Observatory (TO) rural background monitoring station in central Europe, Germany. We used liquid extraction followed by UHPLC-HRMS measurements and NTA for the identification of unknown compounds. Fragmentation spectra comparison with the aerosolomics database[16] enables us to differentiate between anthropogenic and biogenic compounds. HCA, back trajectories and the analysis of the seasonality support data interpretation. This approach could be valuable for understanding the variability and complexity of SOA processes and origins, helping to estimate anthropogenic influences on SOA formation, and thus for validating the anthropogenic aerosol forcing in Earth system models (ESM).

2 Methods

2.1 Ambient aerosol filter sampling

We collected $PM_{2.5}$ filter samples at the Taunus Observatory on top of Kleiner Feldberg (50.222°N, 8.446°E). This rural background monitoring station is located 20 km north-west of downtown Frankfurt, Germany. Previously baked (450 °C for 12 hours) glass fiber filters (150 mm, Ahlstrom-Munksjö) were sampled for 12 hours each, starting at 06:00 UTC and 18:00 UTC, respectively, using a high-volume sampler (HVS DHA-80, Digitel Elektronik AG) at a flow rate of 30 $m^3\ h^{-1}$. Weekly field blanks were stored inside the housing of the HVS without sampling. All filters were wrapped in aluminium foil and stored at −18 °C. Meteorological parameters, PM and trace gas concentrations were provided by the German Weather Service (DWD)[25] and the Hessian Agency for Nature Conservation, Environment and Geology (HLNUG).[26] For the sampling period only PM_{10} values were available, which were used for qualitative statements about fine particle concentration due to a good correlation ($R^2 = 0.88$) between $PM_{2.5}$ and PM_{10} between March 2023 and February 2024 (Fig. S1†).

2.2 Sample preparation

We extracted the day and night filters every second day ($n = 352$) as well as the weekly field blanks ($n = 49$) from August 2021 to August 2022 in two steps, with 10% acetonitrile (Optima LC/MS Grade, Thermo Fisher Scientific Inc.) in water (Milli-Q Reference A+, Merck KGaA). One punch (25 mm diameter) was cut into small pieces and extracted for 20 minutes on an orbital shaker with 200 µl in the first step and with 100 µl in the second step. After each step, we filtered the extract with a syringe (Injekt-F, Braun Melsungen AG) and a 0.2 µm filter (non-sterile polytetrafluoroethylene (PTFE) syringe filter, Thermo Fisher Scientific Inc.). 100 µl of the extracts were spiked with 10 µl of isotopically labelled benzoic acid ($C_6H_5{}^{13}CO_2H$, 99 atom% ^{13}C, Sigma-Aldrich, $c = 0.1$ mg ml^{-1}) as an injection standard to control the stability of the measuring system over several measuring phases.

2.3 UHPLC-HRMS measurements

We measured the extracts in full scan MS with data dependent tandem mass spectrometry ($ddMS^2$) on a high-resolution hybrid quadrupole-Orbitrap mass spectrometer (Q Exactive Focus, Thermo Fisher Scientific Inc.) operated with a heated electrospray ionisation source (HESI-II Probe, Thermo Fisher Scientific Inc.) in negative mode. Detailed settings of the MS are given in Table S1.† Separation was performed by ultra-high-performance liquid chromatography (UHPLC Vanquish Flex, Thermo Fisher Scientific Inc.) on a reversed phase column (Cortecs Solid Core T3, 2.7 µm, 150 × 3 mm, with the corresponding VanGuard Cartridge, Waters Corp.). Detailed settings of the UHPLC are provided in Table S2.†

2.4 Oxidation flow reactor experiments

To identify nitrogen-containing compounds, such as organic nitrates, we oxidized α-pinene in the presence of O_3, OH and NO_x (NO + NO_2) in a potential aerosol mass oxidation flow reactor (PAM-OFR, Aerodyne Research Inc.)[27,28] (OFR185-iNO according to Peng and Jimenez[29]). To identify sulfur-containing compounds, isoprene was oxidised with external O_3 and OH in the presence of sulfur dioxide (SO_2) (OFR254-iSO2 adapted to Peng and Jimenez[29]). No biogenic precursors were introduced into the PAM-OFR for blank experiments. We sampled on PTFE-coated glass fiber filters (47 mm, Pallflex

Emfab Filters, Pall) for 4 or 2 hours, extracted half of them as described in Subsection 2.2 and measured them as described in Subsection 2.3. The operating conditions of the PAM-OFR are provided in Table S3.†

2.5 Data processing

For identification of known and unknown compounds we used the NTA software Compound Discoverer 3.3 (Thermo Fisher Scientific Inc.). Compounds were identified based on *m*/*z*, retention time, signal intensity, isotopic fine structure, fragmentation spectrum and peak factor. Intensities were corrected with the corresponding weekly filter blank. Compounds were assigned to the aerosolomics database if the fragmentation spectra match factor was > 80%. For multiple hits, we considered assignments with a tolerance of 5%. From those we keep the one with the highest relative abundance in the respective system. The entire workflow is given in Table S4.† Levels of confidence according to Schymanski *et al.*[30] were used for compound identification. Based on a calibration of SOA relevant compounds on the UHPLC-HRMS, we estimate a limit of detection of approximately 10 pg injected on the column based on Küster and Thiel.[31] However, this estimate is only based on the measurement of 8 analytical standards and therefore cannot be applied to all compounds.

For hierarchical clustering we used the blank-corrected data matrix. Euclidean distance metrics and the Ward algorithm were used within the Matlab (R2020a) clustergram function to compute the distance between clusters.

We used the concentration-weighted trajectory (CWT) analysis in ZeFir v3.7 (ref. 32) in combination with the Hybrid Single-Particle Lagrangian Integrated Trajectory (HYSPLIT) model[33] for geographical origin analysis of atmospheric pollution. We calculated 5 days (120 h) back trajectories starting every hour at TO (50.22°N, 8.45°E, 600 m-AGL) using meteorological data from the Global Data Assimilation System (GDAS)[34] with a resolution of 1° × 1°. Detailed settings of the HYSPLIT model and ZeFir are given in Table S5.†

2.6 Quality assurance and control

For quality assurance and control (QA/QC), we regularly measured a mixture of ten organic compounds that cover a wide range of ambient expectable molecular weights (139–311 Da), polarity (retention time from 1.6 to 15 min) and peak intensities (10^7–10^9). The mean relative standard deviation of the peak intensity is 11.9% (Fig. S2†). Based on the retention time assignment node of Compound Discoverer, the mean variability of retention time can be estimated to be less than 6 seconds. The analysis of the injection standard confirms the stability of the measuring system during the three measurement phases.

3 Results and discussion

The NTA on the full-year data set detected 6080 compounds that were significantly different from the blank, defined as a sample-to-blank ratio larger than 5 in at least one sample and the corresponding blank. Of these, 4954 have a predicted composition: 2308 compounds contain the basic structure of carbon, hydrogen and oxygen (CHO, 38%), 1122 compounds contain sulfur (CHOS, 18%), 857 compounds contain nitrogen (CHNO, 14%), 502 compounds contain nitrogen and sulfur (CHNOS, 8%) and 165 compounds are not classified in any of these groups (other, 3%), mainly because of the presence of bromine and chlorine in their composition. 1126 compounds remained without a predicted composition (unidentified, 19%). However, this group plays a minor role, with about 6% of the average intensity. We identified organosulfates and -sulfonates (OSs) by the presence of HSO_4^- (*m*/*z* 96.9601) or SO_3^- (*m*/*z* 79.9574) in

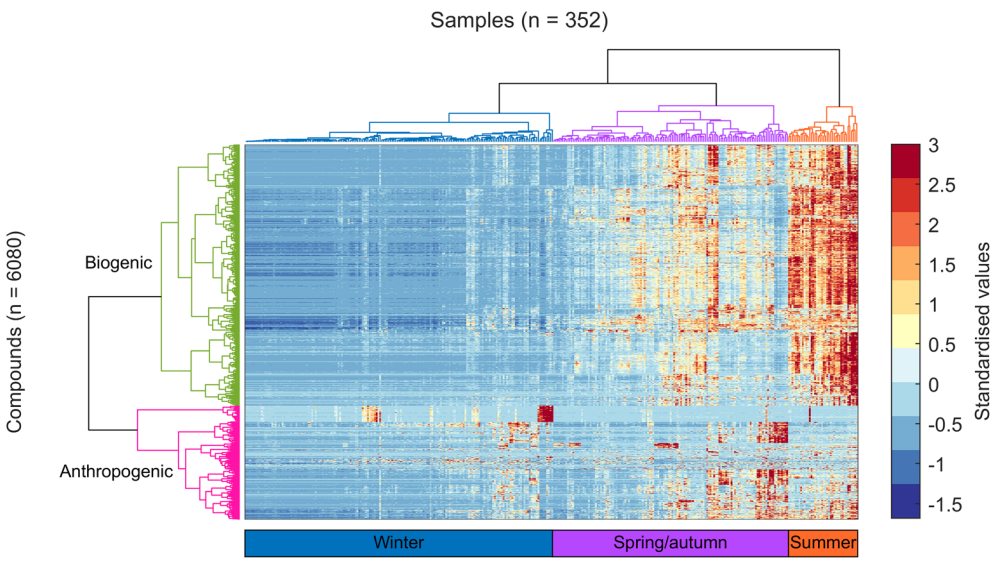

Fig. 1 Heatmap and dendrograms of the HCA. 6080 Compounds are clustered on the *y*-axis, 352 samples on the *x*-axis. The dendrogram of compound clusters are coloured green (biogenic) and magenta (anthropogenic), while the sample clusters are coloured blue (winter), purple (spring/autumn) and orange (summer).

the fragmentation patterns and nitrooxy-organosulfates (NOS) by the additional presence of NO_3^- (m/z 61.9884).

Based on the signal intensities of each compound in each of the 352 filter samples, the HCA (Fig. 1) groups compounds that have a similar trend over time and groups samples that have a similar composition. The longer the connection between two linked dendrograms, the more the chemical composition of the clusters differ from each other. The HCA divided the compounds into two main clusters. Based on the chemical composition, we interpret these clusters as the biogenic compound cluster CI (green) and the anthropogenic compound cluster CII (magenta). Sample clusters were divided into three clusters: the winter sample cluster SI (blue) with a mean temperature ($\bar{T}$) of 2.2 °C and a mean PM mass concentration ($\overline{PM}$) of 5.5 μg m^{-3}, the spring/autumn sample cluster SII (purple, $\bar{T}$ = 10.9 °C, $\overline{PM}$ = 11.4 μg m^{-3}) and the summer sample cluster SIII (orange, $\bar{T}$ = 19.2 °C, $\overline{PM}$ = 14.2 μg m^{-3}) (Fig. S3†). Despite the measurement of day and night filters, no evidence of a diurnal cycle was identified in the clustering. This likely reflects the stronger influence of long-range transported organic aerosol rather than local sources with a diurnal pattern at TO.

The total MS signal intensity shows high variability (Fig. 2a), likely caused by meteorological conditions. We are aware that signal intensities of compounds in the biogenic and anthropogenic cluster are not easily compared to the quantitative measurements of PM mass concentrations due to large differences in ionisation and transmission efficiencies.[24,35] Nevertheless, the strong correlation between the MS signal intensity and PM mass supports our hypothesis: anthropogenic compounds constitute a large fraction of SOA during winter, whereas SOA from biogenic compounds dominate warmer periods with clearly higher fractions (Fig. 2b). To investigate the influence of inorganic aerosol (*e.g.* Saharan dust), we used level 2.0 data from the sun photometer measurements of the Aerosol Robotic Network (AERONET Version 3;[36,37] pre- and post-field calibration applied, cloud-screened and quality-assured data) station at Mainz (Max Planck Institute for Chemistry), 30 km south-west of TO. A clear increase of the coarse mode contribution to the total aerosol could only be detected on 21 March 2022. However, it should be noted that there are some gaps in the data.

3.1 Biogenic compound cluster CI

Compound cluster CI includes 4237 compounds, of which 3378 have a predicted composition (Fig. 3, top panel). These compounds can be assigned to CHO (n = 1873), CHOS (n = 811), CHNO (n = 353), CHNOS (n = 253), other (n = 88) or unidentified (n = 859). They account for 65.8%, 16.6%, 1.7%, 10.0%, 0.3% and 5.6% of the mean signal intensity, respectively. The orbital circles in Fig. 3 are the superposition of several isomers with different intensities, which can be distinguished by different retention times.

CHO compounds predominately have molecular masses between 100 and 300 Da and cover a wide range in retention time (Fig. S4a†). The carbon number is < 20, whereby for compounds with high signal intensities it is mainly 4–10. The average carbon oxidation state ($\overline{OS_c}$) is negative for compounds with carbon number > 10 and follows the trend of atmospheric oxidation and fragmentation, as described in Kroll *et al.*,[38] to positive values for compounds with lower carbon number (Fig. 3a). Biogenic SOA appears at H/C between 1 and 2 (ref. 39) (Fig. 3b), since it is mainly based on isoprenoids, which have

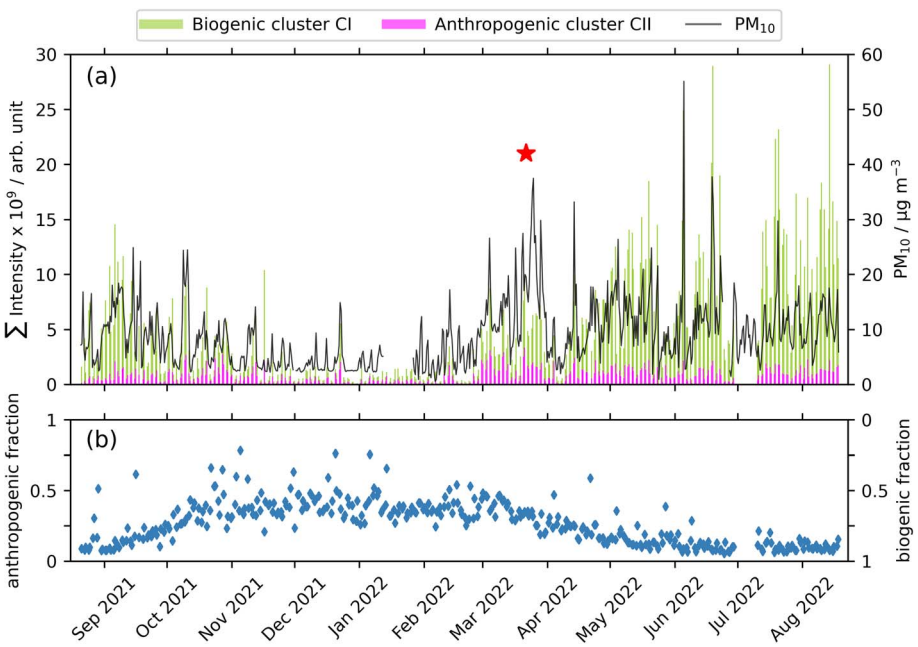

Fig. 2 Time series of the PM_{10} mass concentration, the cumulative MS signal intensities of compounds appearing in cluster CI and cluster CII (a) as well as the ratio of these signal intensities (b). The red star marks a Saharan dust event which was confirmed by the AERONET data as well as back trajectories.

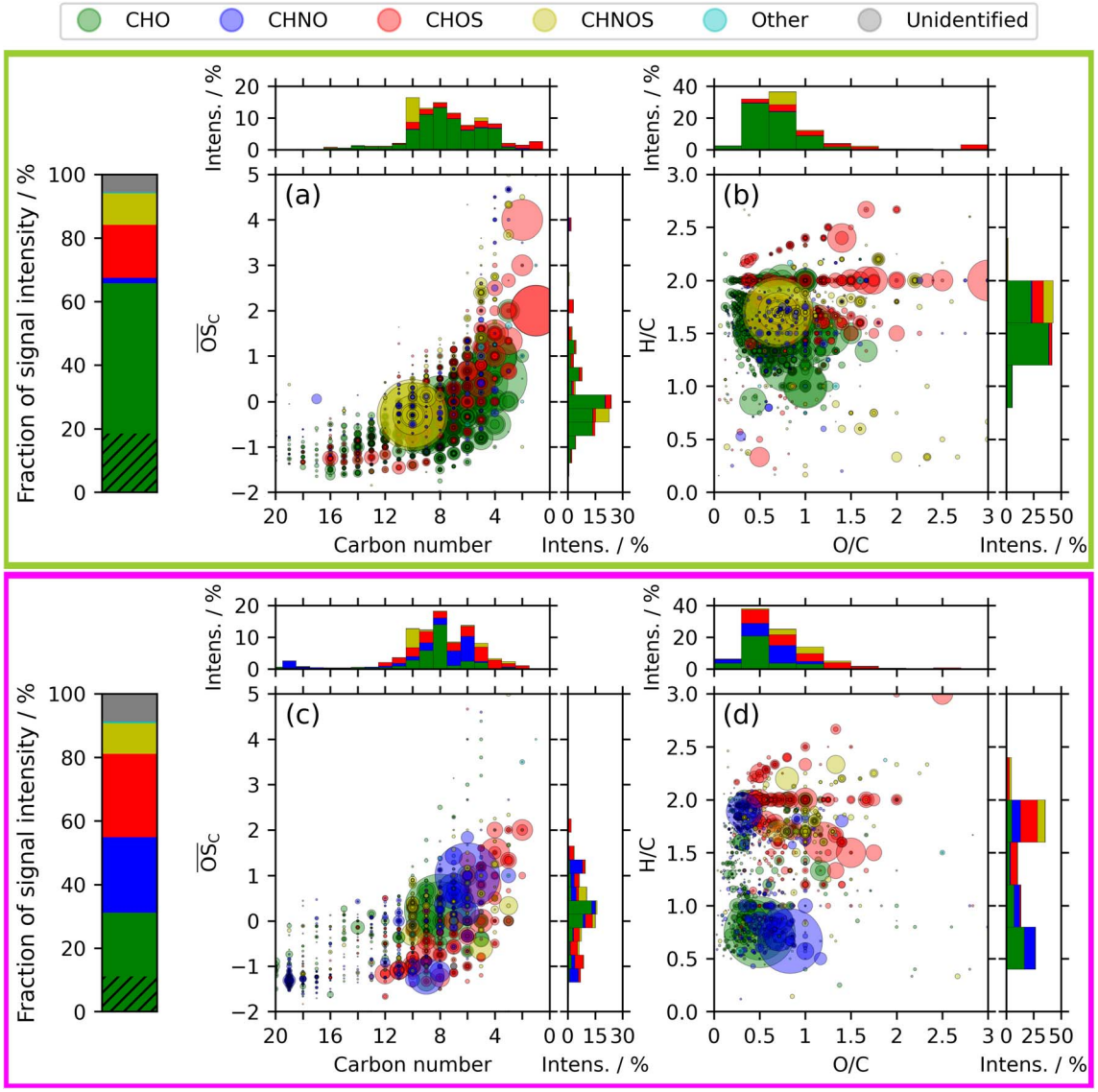

Fig. 3 Chemical fingerprints of compounds from the biogenic (top, green bordered) and the anthropogenic compound cluster (bottom, magenta bordered) illustrated as Kroll plot (a and c) and van Krevelen diagram (b and d). The colour of each scatter indicates the compound class, and the size represents the signal intensity on a linear scale. The bar charts show the cumulative signal intensities for each compound class. The hatched area of the CHO compound class can be assigned to the aerosolomics database.

H/C values of 1.6. The presence of a seasonal cycle with distinct higher signal intensities in summer and lower intensities in winter confirms this hypothesis (Fig. 1), since precursor emissions are highest in summer.[40] Furthermore, we identified 112 CHO compounds with our aerosolomics database, in which the retention times and the fragmentation patterns of different biogenic and anthropogenic SOA compounds are stored. Fig. S5† shows the detailed chemical fingerprint of the CHO compound class for assigned and non-assigned compounds. The 112 identified compounds, which represent 28% of the mean CHO signal intensity, were predominately assigned to biogenic precursors (Fig. S6a†). However, a few compounds were assigned to xylene and trimethylbenzene: those compounds are tentatively small (di-)carboxylic acids, which are not particularly specific tracers, due to their occurrence in both biogenic and anthropogenic oxidation systems. The carbon number (4 and 5) and the loss of CO_2 (m/z 43.9898) in the fragmentation patterns, which is typical for carboxylic acids,[41] supports this interpretation. In this study we interpret isoprene and monoterpenes as purely of biogenic origin due to the location position inside a spacious forest area. Nevertheless, it should be noted that isoprene and monoterpenes can have anthropogenic sources, especially in urban areas.[42,43]

CHOS compounds in compound cluster CI can be divided in two groups. One group contains compounds with high molecular isomers of the homologous series with the general sum formulas $C_nH_{2n+2}O_4S$ (n = 9–13) and $C_nH_{2n}O_5S$ (n = 12–15). The other group contains compounds with wide ranges in mass and retention time. They have mainly carbon number < 10. These compounds are more oxidised (mainly $\overline{OS}_c > 0$) compared to the

compounds of the homologous series ($\overline{OS}_c < -1$). Among them we found the most intense isoprene organosulfates ($C_5H_{12}O_7S$ and $C_2H_4O_6S$) from the PAM-OFR experiments. In May 2022 (SII-a), CWT revealed high intensities for compounds of cluster CI-a (Fig. S7†), indicating the North Sea as a potential source region (Fig. 4a). During this time, the phytoplankton spring bloom takes place in the North Sea.[44] Dimethyl sulfide (CH_3SCH_3) and methanethiol (CH_3SH) are emitted from the ocean and oxidised to SO_2.[45] In combination with biogenic precursors emissions over land, this may lead to the formation of biogenic CHOS compounds.[46,47] Methane sulfonic acid (MSA, CH_3SO_3H), a tracer for marine aerosol,[48] also appears in cluster CI and shows a better correlation with OSs from cluster CI-a ($R^2 = 0.4$) compared to OSs from cluster CII ($R^2 = 0.08$) (Fig. S8†). The increased formation of SOA from biogenic VOCs in the presence of anthropogenic inorganic trace gases, such as NO_x and SO_2,[49,50] results in the oxidation products assuming a biogenic character. Consequently, they are grouped into the biogenic cluster. In addition to biogenic marine sources, SO_2 can also have anthropogenic marine sources such as the burning of heavy fuel oil on ships[51] or oil- and gas-drilling activities in the North Sea. Qi *et al.*[52] show that ports can be a source of SO_2 as well as long-chain alkanes which than can form the high-molecular isomers observed in this cluster. The reason the HCA assigns these compounds into the biogenic cluster is not clear and shows a potential limitation of the HCA, in that further information such as CWT is needed for interpretation of the results.

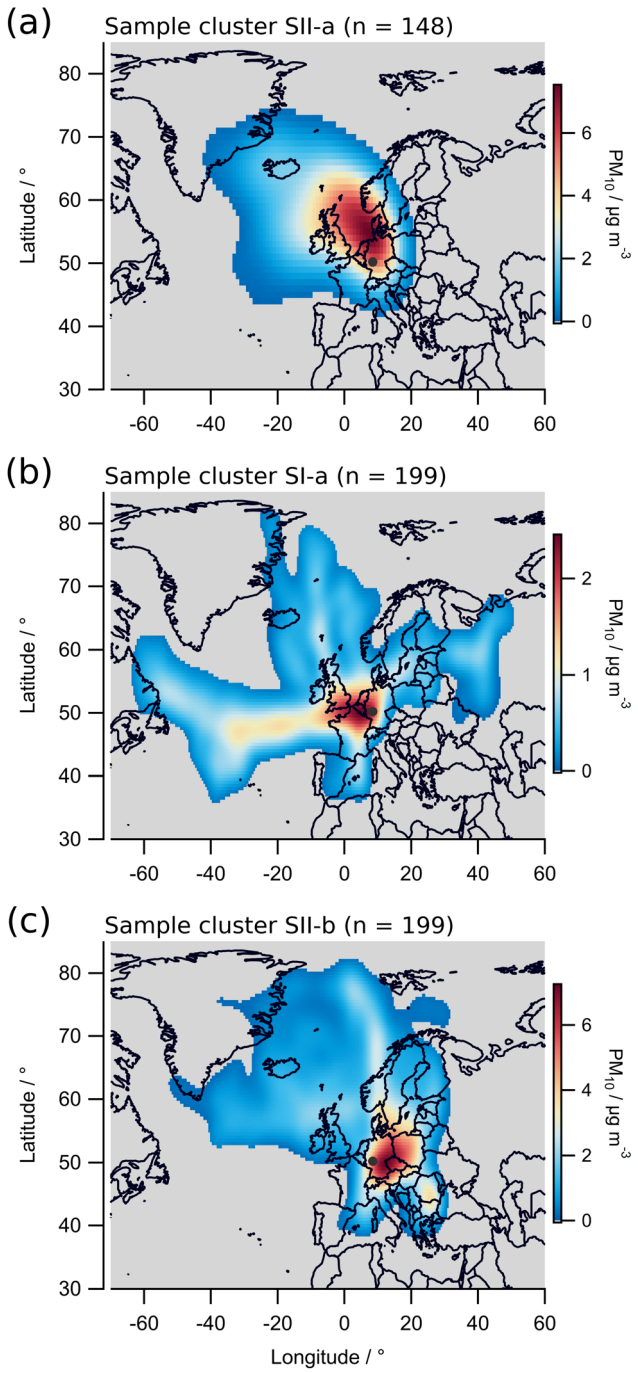

Fig. 4 Concentration weighted trajectories (PM_{10}) of sample clusters SII-a (a), SI-a (b) and SII-b (c) when compounds of clusters CI-a, CII-a and CII-c show high standardised values in the HCA. The CWTs are calculated using n trajectories and PM measurement data.

Although the number of CHNO compounds is higher compared to CHNOS compounds, their intensities are negligible. CHNOS compounds are dominated by several isomers of $C_{10}H_{17}NO_7S$, which are well-characterised NOS derived from monoterpenes.[47] In addition, there are some potential isoprene NOS in the cluster, including $C_5H_{11}NO_8S$ and $C_5H_{11}NO_9S$ described by Surratt *et al.*[53]

3.2 Anthropogenic compound cluster CII

Compound cluster CII consists of 1843 compounds, of which 1576 have a predicted composition (Fig. 3, bottom panel). These compounds have compositions of CHNO ($n = 504$), CHO ($n = 435$), CHOS ($n = 311$), CHNOS ($n = 249$), other ($n = 77$) and unidentified ($n = 267$). They account for 23.7%, 31.2%, 26.3%, 9.7%, 0.5% and 8.7% of the mean signal intensity, respectively.

CHNO compounds have molecular masses of up to 400 Da and retention times above 8 minutes, indicating a low polarity. High signal intensity compounds have a carbon number of 6 or 7 (Fig. 3c) and H/C < 1 (Fig. 3d), indicating nitro-aromatics, tracer compounds for anthropogenic activities (*e.g.* fossil fuel combustion or biomass burning).[54–56] Based on fragmentation patterns we identified dinitrophenol ($C_6H_4N_2O_5$, level 2), nitrosalicylic acid ($C_7H_5NO_5$, level 3), dinitrocresol ($C_7H_6N_2O_5$, level 2), nitrophenol ($C_6H_5NO_3$, level 2) and dinitrosalicylic acid ($C_7H_4N_2O_7$, level 3).

Subcluster CII-a consists almost exclusively of CHNO compounds, which have clearly increased intensities during sample cluster SI-a (Fig. S7†). This sample cluster contains 8 samples, of which 5 are night samples and 3 are day samples. 5 Samples were collected in autumn and one each in summer, winter and spring. Ng *et al.*[57] summarise that organic nitrates can play an important role in SOA formation, especially in regions with high BVOC and NO_x emissions. The CWT shows a widespread origin of air masses with strong local influences, especially west of TO, including heavily populated and industrialised regions like the Ruhr area (Germany), Benelux, north-

eastern France and the southern United Kingdom (Fig. 4b). Anthropogenic emissions, here especially NO_x, can potentially enhance the SOA formation from biogenic precursors.[58] Based on PAM-OFR experiments (subsection 2.4) we can describe 69 compounds of 237 as α-pinene oxidation products under NO_x conditions (Fig. S9†). The compounds were identified by matching retention time and exact mass-to-charge ratio. We suspect that oxidation products of other monoterpenes in the presence of NO_x are the most likely candidates to explain the missing identifications.

In contrast to cluster CI, most CHO compounds have an aromatic character with H/C < 1 (Fig. 3d), indicating anthropogenic SOA. With the aerosolomics database we identified 8 compounds representing 36% of the mean CHO signal intensity, of which 6 are from anthropogenic precursors (Fig. S6b†). Among them are isomers of phthalic acid ($C_8H_6O_4$, level 1) and $C_9H_8O_4$ (level 2, aerosolomics precursor VOC: 1,2,4-trimethylbenzene), a compound also found in the PM of an industrial city[59] as well as in PM of chamber experiments with indene.[60]

The homologous series $C_nH_{2n}O_4S$ ($n = 2$–9), $C_nH_{2n+2}O_4S$ ($n = 2$–10), $C_nH_{2n}O_5S$ ($n = 3$–13), $C_nH_{2n-2}O_5S$ ($n = 3$–11), $C_nH_{2n}O_6S$ ($n = 3$–11) and $C_nH_{2n-2}O_6S$ ($n = 4$–10) is composed of alkyl-organosulfates with double bond equivalents ($\mathrm{DBE} = c - \frac{h}{2} - \frac{n}{2} + 1$, for $C_cH_hN_nO_o$) between 0 and 2, strongly indicating fossil fuel combustion as potential SOA sources.[61]

Compounds which are attributed to anthropogenic activities, appearing in CII-b (mainly aromatic CHO and CHNO) and CII-c (mainly aliphatic CHOS and CHNOS), show high values at the first two weeks of March 2022, whereas compounds from CI and CII-a show very low values (Fig. S7, SII-b†). This period is characterised by stable, warm and dry weather conditions in Europe,[62] which enable long-range transport of aerosols. The CWT highlight eastern Germany, the Czech Republic, southern Poland and somewhat smaller sources including the Balkans as the potential origins of PM (Fig. 4c). The many coal-fired power plants located in these regions are a plausible source of anthropogenic compounds.

4 Conclusions

We investigated the chemical composition of a one-year data set from $PM_{2.5}$ filter samples, collected at a rural background monitoring station in central Europe. The hierarchical cluster analysis grouped the 6080 detected compounds into two main clusters. Based on the molecular composition, seasonal distribution, fragmentation spectra comparison and concentration-weighted trajectories, we classified the compounds therein to be of biogenic and anthropogenic origin. Although the measurements are not quantitative, the strong correlation between the mass spectrometer's intensity and PM mass concentration suggests that biogenic SOA dominates PM variability during summer. With lower PM mass concentrations during winter, we find a higher fraction of anthropogenic OA, reaching up to half of the total signal.

Biogenic compounds show their highest intensities in summer, coinciding with the peak BVOC emissions. Comparison of the fragmentation spectra with the aerosolomics database further supports their classification as a biogenic cluster. The composition of two sub-clusters highlights the importance of multiphase reactions between biogenic precursors and anthropogenic trace gases. Volatile oxidation products of small precursors (*e.g.* isoprene) remain in the gas phase until multiphase reactions involving sulfuric acid reduce the volatility and thus increase the SOA yield.[63,64] As the carbon in the resulting compounds may be partly biogenic in origin, these compounds are clustered into the biogenic cluster.

The anthropogenic compound cluster is strongly influenced by nitro-aromatics and sulfur-containing oxygenated aliphatic hydrocarbons, which are markers for fossil fuel combustion. Most CHO compounds have H/C < 1, implying aromatic structures. The fragmentation spectra comparison with the aerosolomics database results in mostly anthropogenic compounds. Compared to biogenic compounds, anthropogenic compounds are less variable and do not show a clear seasonal cycle.

The large impact of PM on health and climate as well as the uncertainties involved highlight the need for a deeper and more comprehensive characterisation of SOA at the molecular level to better understand their sources, transformation pathways and contribution to the PM loading. With the here presented experimental approach, we are now able to attribute organic compounds to either biogenic or anthropogenic sources on a qualitative basis. To quantify the individual contribution to total OA, one should strive for complementary co-located measurements by offline UHPLC-HRMS and online aerosol mass spectrometer or aerosol chemical speciation monitor at multiple sites to validate ESMs towards the anthropogenic fraction in ambient OA.

Data availability

Data for this article, including the non-target analysis results, are available at Goethe University Data Repository (GUDe) at **https://doi.org/10.25716/gude.06z5-v0gs**.

Author contributions

Conceptualization: MT, FB, ALV; data curation: MT, FB; formal analysis: MT; funding acquisition: ALV; investigation: MT, FB, KK, JD, MS, ALV; methodology: MT, FB, ALV; project administration: ALV; resources: ALV; software: MT, FB; supervision: ALV; validation: MT, FB, JD; visualization: MT, FB, MS, JD, ALV; writing – original draft: MT, ALV; writing – review & editing: all authors.

Conflicts of interest

There are no conflicts to declare.

Acknowledgements

This research has been supported by the Deutsche Forschungsgemeinschaft (DFG; German Research Foundation; grant no. 410009325 and 428312742 (TRR 301)). We thank

Diana Rose (HLNUG) for data support of PM measurements at Taunus Observatory, Meinrat O. Andreae for its effort in establishing and maintaining AERONET Mainz site, Florian Ungeheuer and Robin Klimek for synthesis support and Vaios Moschos for providing support with ZeFir.

References

1 M. Shrivastava, C. D. Cappa, J. Fan, A. H. Goldstein, A. B. Guenther, J. L. Jimenez, C. Kuang, A. Laskin, S. T. Martin, N. L. Ng, T. Petaja, J. R. Pierce, P. J. Rasch, P. Roldin, J. H. Seinfeld, J. Shilling, J. N. Smith, J. A. Thornton, R. Volkamer, J. Wang, D. R. Worsnop, R. A. Zaveri, A. Zelenyuk and Q. Zhang, Recent advances in understanding secondary organic aerosol: Implications for global climate forcing, *Rev. Geophys.*, 2017, **55**, 509–559.

2 Intergovernmental Panel On Climate Change (IPCC), *Climate Change 2021 – The Physical Science Basis: Working Group I Contribution to the Sixth Assessment Report of the Intergovernmental Panel on Climate Change*, Cambridge University Press, 1st edn, 2023.

3 W. Fan, T. Chen, Z. Zhu, H. Zhang, Y. Qiu and D. Yin, A review of secondary organic aerosols formation focusing on organosulfates and organic nitrates, *J. Hazard. Mater.*, 2022, **430**, 128406.

4 World Health Organization, *WHO Global Air Quality Guidelines. Particulate Matter (PM2.5and PM10), Ozone, Nitrogen Dioxide, Sulfur Dioxide and Carbon Monoxide*, World Health Organization, 2021.

5 H. Yin, M. Brauer, J. (Jim) Zhang, W. Cai, S. Navrud, R. Burnett, C. Howard, Z. Deng, D. M. Kammen, H. J. Schellnhuber, K. Chen, H. Kan, Z.-M. Chen, B. Chen, N. Zhang, Z. Mi, D. Coffman, A. J. Cohen, D. Guan, Q. Zhang, P. Gong and Z. Liu, Population ageing and deaths attributable to ambient $PM_{2.5}$ pollution: a global analysis of economic cost, *Lancet Planet. Health*, 2021, **5**, 356–367.

6 World Bank Group, *The Cost of Air Pollution – Strengthening the Economic Case for Action*, World Bank Group, 2016.

7 J. L. Jimenez, M. R. Canagaratna, N. M. Donahue, A. S. H. Prevot, Q. Zhang, J. H. Kroll, P. F. DeCarlo, J. D. Allan, H. Coe, N. L. Ng, A. C. Aiken, K. S. Docherty, I. M. Ulbrich, A. P. Grieshop, A. L. Robinson, J. Duplissy, J. D. Smith, K. R. Wilson, V. A. Lanz, C. Hueglin, Y. L. Sun, J. Tian, A. Laaksonen, T. Raatikainen, J. Rautiainen, P. Vaattovaara, M. Ehn, M. Kulmala, J. M. Tomlinson, D. R. Collins, M. J. Cubison, E. J. Dunlea, J. A. Huffman, T. B. Onasch, M. R. Alfarra, P. I. Williams, K. Bower, Y. Kondo, J. Schneider, F. Drewnick, S. Borrmann, S. Weimer, K. Demerjian, D. Salcedo, L. Cottrell, R. Griffin, A. Takami, T. Miyoshi, S. Hatakeyama, A. Shimono, J. Y. Sun, Y. M. Zhang, K. Dzepina, J. R. Kimmel, D. Sueper, J. T. Jayne, S. C. Herndon, A. M. Trimborn, L. R. Williams, E. C. Wood, A. M. Middlebrook, C. E. Kolb, U. Baltensperger and D. R. Worsnop, Evolution of Organic Aerosols in the Atmosphere, *Science*, 2009, **326**, 1525–1529.

8 R. Atkinson and J. Arey, Atmospheric Degradation of Volatile Organic Compounds, *Chem. Rev.*, 2003, **103**, 4605–4638.

9 G. Chen, F. Canonaco, A. Tobler, W. Aas, A. Alastuey, J. Allan, S. Atabakhsh, M. Aurela, U. Baltensperger, A. Bougiatioti, J. F. De Brito, D. Ceburnis, B. Chazeau, H. Chebaicheb, K. R. Daellenbach, M. Ehn, I. El Haddad, K. Eleftheriadis, O. Favez, H. Flentje, A. Font, K. Fossum, E. Freney, M. Gini, D. C. Green, L. Heikkinen, H. Herrmann, A.-C. Kalogridis, H. Keernik, R. Lhotka, C. Lin, C. Lunder, M. Maasikmets, M. I. Manousakas, N. Marchand, C. Marin, L. Marmureanu, N. Mihalopoulos, G. Močnik, J. Nęcki, C. O'Dowd, J. Ovadnevaite, T. Peter, J.-E. Petit, M. Pikridas, S. Matthew Platt, P. Pokorná, L. Poulain, M. Priestman, V. Riffault, M. Rinaldi, K. Różański, J. Schwarz, J. Sciare, L. Simon, A. Skiba, J. G. Slowik, Y. Sosedova, I. Stavroulas, K. Styszko, E. Teinemaa, H. Timonen, A. Tremper, J. Vasilescu, M. Via, P. Vodička, A. Wiedensohler, O. Zografou, M. Cruz Minguillón and A. S. H. Prévôt, European aerosol phenomenology – 8: Harmonised source apportionment of organic aerosol using 22 Year-long ACSM/AMS datasets, *Environ. Int.*, 2022, **166**, 107325.

10 Y.-L. Zhang, I. El-Haddad, R.-J. Huang, K.-F. Ho, J.-J. Cao, Y. Han, P. Zotter, C. Bozzetti, K. R. Daellenbach, J. G. Slowik, G. Salazar, A. S. H. Prévôt and S. Szidat, Large contribution of fossil fuel derived secondary organic carbon to water soluble organic aerosols in winter haze in China, *Atmos. Chem. Phys.*, 2018, **18**, 4005–4017.

11 J. Wei, L. Xiang and Z. Cai, Emerging environmental pollutants hydroxylated polybrominated diphenyl ethers: From analytical methods to toxicology research, *Mass Spectrom. Rev.*, 2021, **40**, 255–279.

12 Y. Chen, M. Takeuchi, T. Nah, L. Xu, M. R. Canagaratna, H. Stark, K. Baumann, F. Canonaco, A. S. H. Prévôt, L. G. Huey, R. J. Weber and N. L. Ng, Chemical characterization of secondary organic aerosol at a rural site in the southeastern US: insights from simultaneous high-resolution time-of-flight aerosol mass spectrometer (HR-ToF-AMS) and FIGAERO chemical ionization mass spectrometer (CIMS) measurements, *Atmos. Chem. Phys.*, 2020, **20**, 8421–8440.

13 P. Patel, S. G. Aggarwal, C.-J. Tsai and T. Okuda, Theoretical and field evaluation of a $PM_{2.5}$ high-volume impactor inlet design, *Atmos. Environ.*, 2021, **244**, 117811.

14 K. E. Manz, A. Feerick, J. M. Braun, Y.-L. Feng, A. Hall, J. Koelmel, C. Manzano, S. R. Newton, K. D. Pennell, B. J. Place, K. J. Godri Pollitt, C. Prasse and J. A. Young, Non-targeted analysis (NTA) and suspect screening analysis (SSA): a review of examining the chemical exposome, *J. Exposure Sci. Environ. Epidemiol.*, 2023, **33**, 524–536.

15 HichChem LLC, mzCloud Advanced Mass Spectral Database, https://www.mzcloud.org/, accessed 10 December 2024.

16 M. Thoma, F. Bachmeier, F. L. Gottwald, M. Simon and A. L. Vogel, Mass spectrometry-based *Aerosolomics* : a new approach to resolve sources, composition, and partitioning of secondary organic aerosol, *Atmos. Meas. Tech.*, 2022, **15**, 7137–7154.

17 F. Ungeheuer, D. Van Pinxteren and A. L. Vogel, Identification and source attribution of organic compounds in ultrafine particles near Frankfurt International Airport, *Atmos. Chem. Phys.*, 2021, **21**, 3763–3775.
18 A. L. Vogel, A. Lauer, L. Fang, K. Arturi, F. Bachmeier, K. R. Daellenbach, T. Käser, A. Vlachou, V. Pospisilova, U. Baltensperger, I. E. Haddad, M. Schwikowski and S. Bjelić, A Comprehensive Nontarget Analysis for the Molecular Reconstruction of Organic Aerosol Composition from Glacier Ice Cores, *Environ. Sci. Technol.*, 2019, **53**, 12565–12575.
19 J. P. Wallraff, F. Ungeheuer, A. Dombrowski, J. Oehlmann and A. L. Vogel, Occurrence and *in vitro* toxicity of organic compounds in urban background PM2.5, *Sci. Total Environ.*, 2022, **817**, 152779.
20 B. Witkowski, M. al-Sharafi, K. Błaziak and T. Gierczak, Aging of α-Pinene Secondary Organic Aerosol by Hydroxyl Radicals in the Aqueous Phase: Kinetics and Products, *Environ. Sci. Technol.*, 2023, **57**, 6040–6051.
21 H.-A. Synal, M. Stocker and M. Suter, MICADAS: A new compact radiocarbon AMS system, *Nucl. Instrum. Methods Phys. Res., Sect. B*, 2007, **259**, 7–13.
22 S. Szidat, T. M. Jenk, H. W. Gäggeler, H.-A. Synal, R. Fisseha, U. Baltensperger, M. Kalberer, V. Samburova, S. Reimann, A. Kasper-Giebl and I. Hajdas, Radiocarbon (^{14}C)-deduced biogenic and anthropogenic contributions to organic carbon (OC) of urban aerosols from Zürich, Switzerland, *Atmos. Environ.*, 2004, **38**, 4035–4044.
23 S. Szidat, T. M. Jenk, H. W. Gäggeler, H.-A. Synal, I. Hajdas, G. Bonani and M. Saurer, THEODORE, a two-step heating system for the EC/OC determination of radiocarbon (^{14}C) in the environment, *Nucl. Instrum. Methods Phys. Res., Sect. B*, 2004, **223–224**, 829–836.
24 J. Ma, F. Ungeheuer, F. Zheng, W. Du, Y. Wang, J. Cai, Y. Zhou, C. Yan, Y. Liu, M. Kulmala, K. R. Daellenbach and A. L. Vogel, Nontarget Screening Exhibits a Seasonal Cycle of $PM_{2.5}$ Organic Aerosol Composition in Beijing, *Environ. Sci. Technol.*, 2022, **56**, 7017–7028.
25 German Weather Sevice, CDC (Climate Data Center), **https://www.dwd.de/EN/climate_environment/cdc/cdc_node_en.html**, accessed 12 December 2024.
26 Hessian Agency for Nature Conservation, Environment and Geology, Messdatenportal, **https://www.hlnug.de/messwerte/datenportal/messstelle/2/1/0675/**, accessed 12 December 2024.
27 E. Kang, M. J. Root, D. W. Toohey and W. H. Brune, Introducing the concept of Potential Aerosol Mass (PAM), *Atmos. Chem. Phys.*, 2007, **7**, 5727–5744.
28 A. T. Lambe, A. T. Ahern, L. R. Williams, J. G. Slowik, J. P. S. Wong, J. P. D. Abbatt, W. H. Brune, N. L. Ng, J. P. Wright, D. R. Croasdale, D. R. Worsnop, P. Davidovits and T. B. Onasch, Characterization of aerosol photooxidation flow reactors: heterogeneous oxidation, secondary organic aerosol formation and cloud condensation nuclei activity measurements, *Atmos. Meas. Tech.*, 2011, **4**, 445–461.
29 Z. Peng and J. L. Jimenez, Radical chemistry in oxidation flow reactors for atmospheric chemistry research, *Chem. Soc. Rev.*, 2020, **49**, 2570–2616.
30 E. L. Schymanski, J. Jeon, R. Gulde, K. Fenner, M. Ruff, H. P. Singer and J. Hollender, Identifying Small Molecules *via* High Resolution Mass Spectrometry: Communicating Confidence, *Environ. Sci. Technol.*, 2014, **48**, 2097–2098.
31 F. W. Küster and A. Thiel, *Rechentafeln für die Chemische Analytik*, Walter de Gruyter & Co. KG, Berlin, 2008, vol. 106.
32 J.-E. Petit, O. Favez, A. Albinet and F. Canonaco, A user-friendly tool for comprehensive evaluation of the geographical origins of atmospheric pollution: Wind and trajectory analyses, *Environ. Model. Softw.*, 2017, **88**, 183–187.
33 A. F. Stein, R. R. Draxler, G. D. Rolph, B. J. B. Stunder, M. D. Cohen and F. Ngan, NOAA's HYSPLIT Atmospheric Transport and Dispersion Modeling System, *Bull. Am. Meteorol. Soc.*, 2015, **96**, 2059–2077.
34 Environmental Modeling Center and National Centers for Environmental Prediction, National Weather Service, NOAA, and U.S. Department of Commerce, Global Data Assimilation System, **https://www.ready.noaa.gov/data/archives/gdas1/**, accessed 12 December 2024.
35 R. L. Evans, D. J. Bryant, A. Voliotis, D. Hu, H. Wu, S. A. Syafira, O. E. Oghama, G. McFiggans, J. F. Hamilton and A. R. Rickard, A Semi-Quantitative Approach to Nontarget Compositional Analysis of Complex Samples, *Anal. Chem.*, 2024, **96**, 18349–18358.
36 D. M. Giles, A. Sinyuk, M. G. Sorokin, J. S. Schafer, A. Smirnov, I. Slutsker, T. F. Eck, B. N. Holben, J. R. Lewis, J. R. Campbell, E. J. Welton, S. V. Korkin and A. I. Lyapustin, Advancements in the Aerosol Robotic Network (AERONET) Version 3 database – automated near-real-time quality control algorithm with improved cloud screening for Sun photometer aerosol optical depth (AOD) measurements, *Atmos. Meas. Tech.*, 2019, **12**, 169–209.
37 B. N. Holben, T. F. Eck, I. Slutsker, D. Tanré, J. P. Buis, A. Setzer, E. Vermote, J. A. Reagan, Y. J. Kaufman, T. Nakajima, F. Lavenu, I. Jankowiak and A. Smirnov, AERONET—A Federated Instrument Network and Data Archive for Aerosol Characterization, *Rem. Sens. Environ.*, 1998, **66**, 1–16.
38 J. H. Kroll, N. M. Donahue, J. L. Jimenez, S. H. Kessler, M. R. Canagaratna, K. R. Wilson, K. E. Altieri, L. R. Mazzoleni, A. S. Wozniak, H. Bluhm, E. R. Mysak, J. D. Smith, C. E. Kolb and D. R. Worsnop, Carbon oxidation state as a metric for describing the chemistry of atmospheric organic aerosol, *Nat. Chem.*, 2011, **3**, 133–139.
39 K. R. Daellenbach, I. Kourtchev, A. L. Vogel, E. A. Bruns, J. Jiang, T. Petäjä, J.-L. Jaffrezo, S. Aksoyoglu, M. Kalberer, U. Baltensperger, I. El Haddad and A. S. H. Prévôt, Impact of anthropogenic and biogenic sources on the seasonal variation in the molecular composition of urban organic aerosols: a field and laboratory study using ultra-high-resolution mass spectrometry, *Atmos. Chem. Phys.*, 2019, **19**, 5973–5991.
40 D. Helmig, R. W. Daly, J. Milford and A. Guenther, Seasonal trends of biogenic terpene emissions, *Chemosphere*, 2013, **93**, 35–46.

41 M. L. Bandu, K. R. Watkins, M. L. Bretthauer, C. A. Moore and H. Desaire, Prediction of MS/MS Data. 1. A Focus on Pharmaceuticals Containing Carboxylic Acids, *Anal. Chem.*, 2004, **76**, 1746–1753.

42 G. I. Gkatzelis, M. M. Coggon, B. C. McDonald, J. Peischl, J. B. Gilman, K. C. Aikin, M. A. Robinson, F. Canonaco, A. S. H. Prevot, M. Trainer and C. Warneke, Observations Confirm that Volatile Chemical Products Are a Major Source of Petrochemical Emissions in U.S. Cities, *Environ. Sci. Technol.*, 2021, **55**, 4332–4343.

43 D. J. Bryant, B. S. Nelson, S. J. Swift, S. H. Budisulistiorini, W. S. Drysdale, A. R. Vaughan, M. J. Newland, J. R. Hopkins, J. M. Cash, B. Langford, E. Nemitz, W. J. F. Acton, C. N. Hewitt, T. Mandal, B. R. Gurjar, Shivani, R. Gadi, J. D. Lee, A. R. Rickard and J. F. Hamilton, Biogenic and anthropogenic sources of isoprene and monoterpenes and their secondary organic aerosol in Delhi, India, *Atmos. Chem. Phys.*, 2023, **23**, 61–83.

44 R. González-Gil, N. S. Banas, E. Bresnan and M. R. Heath, The onset of the spring phytoplankton bloom in the coastal North Sea supports the Disturbance Recovery Hypothesis, *Biogeosciences*, 2022, **19**, 2417–2426.

45 G. A. Novak, D. B. Kilgour, C. M. Jernigan, M. P. Vermeuel and T. H. Bertram, Oceanic emissions of dimethyl sulfide and methanethiol and their contribution to sulfur dioxide production in the marine atmosphere, *Atmos. Chem. Phys.*, 2022, **22**, 6309–6325.

46 M. Brüggemann, D. Van Pinxteren, Y. Wang, J. Z. Yu and H. Herrmann, Quantification of known and unknown terpenoid organosulfates in PM10 using untargeted LC–HRMS/MS: contrasting summertime rural Germany and the North China Plain, *Environ. Chem.*, 2019, **16**, 333–346.

47 J. D. Surratt, Y. Gómez-González, A. W. H. Chan, R. Vermeylen, M. Shahgholi, T. E. Kleindienst, E. O. Edney, J. H. Offenberg, M. Lewandowski, M. Jaoui, W. Maenhaut, M. Claeys, R. C. Flagan and J. H. Seinfeld, Organosulfate Formation in Biogenic Secondary Organic Aerosol, *J. Phys. Chem. A*, 2008, **112**, 8345–8378.

48 E. S. Saltzman, D. L. Savoie, R. G. Zika and J. M. Prospero, Methane sulfonic acid in the marine atmosphere, *J. Geophys. Res.*, 1983, **88**, 10897–10902.

49 C. R. Hoyle, M. Boy, N. M. Donahue, J. L. Fry, M. Glasius, A. Guenther, A. G. Hallar, K. Huff Hartz, M. D. Petters, T. Petäjä, T. Rosenoern and A. P. Sullivan, A review of the anthropogenic influence on biogenic secondary organic aerosol, *Atmos. Chem. Phys.*, 2011, **11**, 321–343.

50 C. M. Stangl, J. M. Krasnomowitz, M. J. Apsokardu, L. Tiszenkel, Q. Ouyang, S. Lee and M. V. Johnston, Sulfur Dioxide Modifies Aerosol Particle Formation and Growth by Ozonolysis of Monoterpenes and Isoprene, *J. Geophys. Res.:Atmos.*, 2019, **124**, 4800–4811.

51 S. Becagli, D. M. Sferlazzo, G. Pace, A. Di Sarra, C. Bommarito, G. Calzolai, C. Ghedini, F. Lucarelli, D. Meloni, F. Monteleone, M. Severi, R. Traversi and R. Udisti, Evidence for heavy fuel oil combustion aerosols from chemical analyses at the island of Lampedusa: a possible large role of ships emissions in the Mediterranean, *Atmos. Chem. Phys.*, 2012, **12**, 3479–3492.

52 L. Qi, Z. Zhang, X. Wang, F. Deng, J. Zhao and H. Liu, Molecular characterization of atmospheric particulate organosulfates in a port environment using ultrahigh resolution mass spectrometry: Identification of traffic emissions, *J. Hazard. Mater.*, 2021, **419**, 126431.

53 J. D. Surratt, J. H. Kroll, T. E. Kleindienst, E. O. Edney, M. Claeys, A. Sorooshian, N. L. Ng, J. H. Offenberg, M. Lewandowski, M. Jaoui, R. C. Flagan and J. H. Seinfeld, Evidence for Organosulfates in Secondary Organic Aerosol, *Environ. Sci. Technol.*, 2007, **41**, 517–527.

54 S. Huang, X. Yang, H. Xu, Y. Zeng, D. Li, J. Sun, S. S. H. Ho, Y. Zhang, J. Cao and Z. Shen, Insights into the nitroaromatic compounds, formation, and light absorption contributing emissions from various geological maturity coals, *Sci. Total Environ.*, 2023, **870**, 162033.

55 V. Moschos, C. Christensen, M. Mouton, M. N. Fiddler, T. Isolabella, F. Mazzei, D. Massabò, B. J. Turpin, S. Bililign and J. D. Surratt, Quantifying the Light-Absorption Properties and Molecular Composition of Brown Carbon Aerosol from Sub-Saharan African Biomass Combustion, *Environ. Sci. Technol.*, 2024, 4268–4280.

56 C. M. G. Salvador, R. Tang, M. Priestley, L. Li, E. Tsiligiannis, M. Le Breton, W. Zhu, L. Zeng, H. Wang, Y. Yu, M. Hu, S. Guo and M. Hallquist, Ambient nitro-aromatic compounds – biomass burning *versus* secondary formation in rural China, *Atmos. Chem. Phys.*, 2021, **21**, 1389–1406.

57 N. L. Ng, S. S. Brown, A. T. Archibald, E. Atlas, R. C. Cohen, J. N. Crowley, D. A. Day, N. M. Donahue, J. L. Fry, H. Fuchs, R. J. Griffin, M. I. Guzman, H. Herrmann, A. Hodzic, Y. Iinuma, J. L. Jimenez, A. Kiendler-Scharr, B. H. Lee, D. J. Luecken, J. Mao, R. McLaren, A. Mutzel, H. D. Osthoff, B. Ouyang, B. Picquet-Varrault, U. Platt, H. O. T. Pye, Y. Rudich, R. H. Schwantes, M. Shiraiwa, J. Stutz, J. A. Thornton, A. Tilgner, B. J. Williams and R. A. Zaveri, Nitrate radicals and biogenic volatile organic compounds: oxidation, mechanisms, and organic aerosol, *Atmos. Chem. Phys.*, 2017, **17**, 2103–2162.

58 M. Shrivastava, M. O. Andreae, P. Artaxo, H. M. J. Barbosa, L. K. Berg, J. Brito, J. Ching, R. C. Easter, J. Fan, J. D. Fast, Z. Feng, J. D. Fuentes, M. Glasius, A. H. Goldstein, E. G. Alves, H. Gomes, D. Gu, A. Guenther, S. H. Jathar, S. Kim, Y. Liu, S. Lou, S. T. Martin, V. F. McNeill, A. Medeiros, S. S. De Sá, J. E. Shilling, S. R. Springston, R. A. F. Souza, J. A. Thornton, G. Isaacman-VanWertz, L. D. Yee, R. Ynoue, R. A. Zaveri, A. Zelenyuk and C. Zhao, Urban pollution greatly enhances formation of natural aerosols over the Amazon rainforest, *Nat. Commun.*, 2019, **10**, 1046.

59 W. Wang, Y. Zhang, B. Jiang, Y. Chen, Y. Song, Y. Tang, C. Dong and Z. Cai, Molecular characterization of organic aerosols in Taiyuan, China: Seasonal variation and source identification, *Sci. Total Environ.*, 2021, **800**, 149419.

60 L. Chiappini, E. Perraudin, N. Maurin, B. Picquet-Varrault, W. Zheng, N. Marchand, B. Temime-Roussel, A. Monod, A. Le Person, F. Bernard, G. Eyglunent, A. Mellouki and

J.-F. Doussin, Secondary Organic Aerosol Formation from Aromatic Alkene Ozonolysis: Influence of the Precursor Structure on Yield, Chemical Composition, and Mechanism, *J. Phys. Chem. A*, 2019, **123**, 1469–1484.

61 Y. Du, H. Che, Z. Bao, Y. Liu, Q. Li, M. Hu, J. Zhou, S. Zhang, X. Yao, Q. Shi, C. Chen, Y. Han, L. Meng, X. Long, X. Qi, C. He and Y. Chen, Characterization of Organosulfates (OSs) in typical urban areas in Eastern China: Source, Process, and Volatility, *Atmos. Res.*, 2024, **301**, 107258.

62 U. Kirsche and A. Friedrich, *The Weather in Germany - March 2022*, German Weather Service, 2022.

63 Y. Iinuma, A. Kahnt, A. Mutzel, O. Böge and H. Herrmann, Ozone-Driven Secondary Organic Aerosol Production Chain, *Environ. Sci. Technol.*, 2013, **47**, 3639–3647.

64 J. D. Surratt, A. W. H. Chan, N. C. Eddingsaas, M. Chan, C. L. Loza, A. J. Kwan, S. P. Hersey, R. C. Flagan, P. O. Wennberg and J. H. Seinfeld, Reactive intermediates revealed in secondary organic aerosol formation from isoprene, *Proc. Natl. Acad. Sci. U.S.A.*, 2010, **107**, 6640–6645.